Rev. Roum. Sci. Techn.– Électrotechn. et Énerg.
Vol. **69**, *4*, pp. 425–430, Bucarest, 2024

IMPLEMENTATION OF VIENNA RECTIFIER WITH SLIDING MODE CONTROL FOR ELECTRIC VEHICLE CHARGING STATIONS

BANUMALAR KOODALSAMY[1], VANAJA NARAYANASWAMY[2], KARTHIKEYAN KRISHNAMOORTHY[3], BHUVANESH ANANTHAN [4,*]

Keywords: Electric vehicle; Charging station; Sliding mode control (SMC); Power factor; Harmonics.

This work recommends using an electric vehicle (EV) charging station employing a Vienna rectifier (VR) with sliding mode control. The Vienna rectifier is preferred for high-power applications due to its reduced harmonic distortion and improved power factor correction. Sliding mode control is used to regulate the rectifier's output voltage and current, allowing for reliable and efficient charging of EVs. The suggested system is modeled, and the simulation outcomes are presented to demonstrate the value of the recommended approach concerning stability, strength, and unexpected responsiveness. The proposed technology is expected to contribute to developing more dependable and effective EV charging stations.

1. INTRODUCTION

Single-phase Vienne rectifier (VR), also known as a single-phase bridge rectifier, is an electronic circuit that converts an alternating current (AC) voltage into a direct current (DC) voltage. A modified Vienna rectifier, a transformer for step-down, a T-LCL filter circuit, and an H bridge inverter for transforming power to DC to alternating current (AC) an improved AC to DC conversion using a VR, a straightforward single-phase control system improved switchover in a VR, and a modified VR. A square wave signal in conjunction with SPWM (sinusoidal pulse width modulation) with source-side synchronization is used for the switching pulse of the H-bridge inverter [1]. The suggested sliding mode controller's (SMC's) sliding surface functionality only requires detecting capacitor voltage and grid current, making it less complex than the present SMC approaches designed for grid-connected VSI. The switching frequency is also reduced using a double-band hysteresis technique [2].

To track the rotor angular speed and the square module of rotor flux of the SPIM subjected to perturbations, a control system based on the block control approach, quasi-continuous SM manifold design, and the second-order SM super-twisting algorithms are proposed. A nonlinear observer utilizing second-order SM algorithms is devised to estimate the rotor flux in an instance of an altering plant parameter [3]. Superior converter dynamics, efficient control of the resultant voltage under rapid load variations, and maintenance of a unity power factor are the key goals of the suggested SMC. At an 800 W load power, the sustained state measurements show a power factor > 0.995 and a total harmonic distortion (THD) of 3%. SMC achieves an 80 ms settling period for a 25% step-change in demand power, which is about 200 ms quicker than the traditional PI control [4].

The Vienna rectifier is an improved power quality ac-dc converter (IPQC) of the unidirectional boost type. The rectifier topology can produce a more significant power factor DC output voltage concerning the AC source voltage. According to the simulation results, AC to DC power conversion is provided by topologies with HCC by modern power quality standards [5]. An analysis is done on a new circuit that uses a Vienna rectifier and a single-phase, two-stage inverter. The inverter comprises a square wave, sinusoidal pulse width modulation (SPWM), and grid synchronization requirements. The novel method showed that the improved power factor of over 0.94 was made possible by the low ripple, low THD below 0.1%, low cost, and simple control [6].

Quasi-Z-source inverters (qZSIs) are employed due to these advantages: single-stage operation, cheaper component rating, continuous input current, and common DC rail. In this study, AC and DC side-controlled grid-connected qZSI are presented. A sliding mode control (SMC)--based controller has been developed for capacitor voltage regulation to ensure a quick and dynamic response for significant fluctuations in source voltage and output demand [7]. The switching regulate term is replaced with a fuzzy system to lessen the chattering condition. Additionally, the compensation regulate term is created based on the estimation of the fuzzy approximation error, which guarantees the closed-loop system's tracking performance [8]. With limited convergence and robustness advantages, a promising control approach for PV systems in a single phase linked to the grid is the 2nd-order sliding mode method. The proposed approach eliminates the chattering issue with SMC [9].

The voltage source converter in a single phase, which controls the frequency and microgrid voltage and harmonic current mitigation, is estimated using the reference source current control based adaptive sliding mode control algorithm. The sliding mode control keeps the system's reference real power in check and maintains the energy balance [10]. High-frequency harmonics tend to flow backward toward the supply side, lowering grid-side power quality. VR's unidirectional design shields the induction heating system from high-frequency harmonics. VR enhances the input supply's power factor and reduces the input current's total harmonic distortion [11].

To approximate comparable management and eliminate the unidentified disturbance, a fuzzy double-hidden layer recurrent neural network is suggested and utilized to suppress harmonics, minimizing the function of components involved in symbol switching. The primary goals of the FDHLRNN are to increase precise control and lower the active power filter's current distortion rate [12]. Phase cancellation occurs when these components are put in the closed circuit to generate the reference current of an inductor in the absence of the impact of ripple. In this instance, there is no ripple impact in the actual current of the inductor.

[1,2] Department of EEE, Mepco Schlenk Engineering College, Sivakasi, India.
[3] Department of EEE, Ramco Institute of Technology, Rajapalayam, India.
[4] Department of EEE, PSN College of Engineering and Technology, Tirunelveli, India.
Emails: kbanumalar@mepcoeng.ac.in , nvanaja@mepcoeng.ac.in , karthikeyank@ritrjpm.ac.in, bhuvanesh.ananthan@psncet.ac.in

DOI: 10.59277/RRST-EE.2024.69.4.10

This study presents the effects on an actual medium voltage (MV) grid in Gračanica of both deregulated and regulated electric vehicle (EV) charging scenarios [13]. Adding a power factor correction (PFC) circuit to the charging stations is suggested to raise the power factor and lower harmonic injection [14]. The single-ended primary-inductor converter (SEPIC), which enables isolation between the load and the electrical network, is responsible for achieving this.

The proposed single-phase VR has a pair of power switches and diodes added, improving the output voltage's controllability [17]. This paper proposes an SMC-based single-phase VR for electric vehicle charging.

2. VIENNA RECTIFIER WITH SLIDING MODE CONTROL

This work proposes the circuit topology of a sliding mode control-based VR in a single phase, as shown in Fig. 1. The rectifier consists of four MOSFETs or IGBTs that are active semiconductor switches, along with four diodes. A voltage stress of Vdc/2 is applied to every semiconductor switch and diode. Two capacitors are linked together in parallel on the result DC side, while two inductors are connected in series on the input AC side.

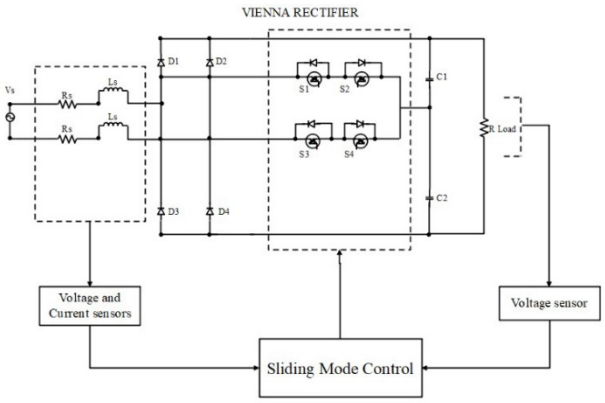

Fig. 1 – Proposed single-phase Vienna rectifier with sliding mode control system.

2.1. VIENNA RECTIFIER

In Mode 1, the controlled switches (MOSFETs) S1, S2, S3, and S4 are switched ON while the diodes D1, D2, D3, and D4 are off. In Fig. 2a, the capacitors C1 and C2 are discharged while the inductors L1 and L2 are charged. The input current is positive. In Mode 2, the toggles S1, S2, S3, and S4 are all switched OFF, while the diode devices D1 and D4 are switched ON. Figure 2b displays the input current while capacitors C1 and C2 charge. When operating in Mode 3, the input current is negative, the switches S1, S2, S3, and S4 are all switched ON, and the diodes D1, D2, D3, and D4 are off. Figure 2c shows the capacitors C1 and C2 discharging and inductors L1 and L2 charging.

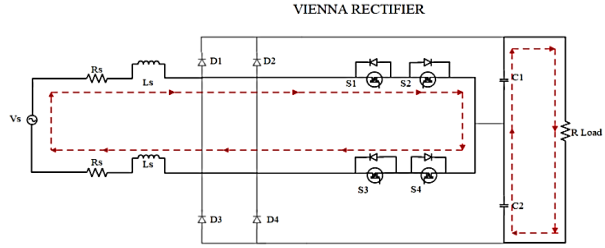

(a)

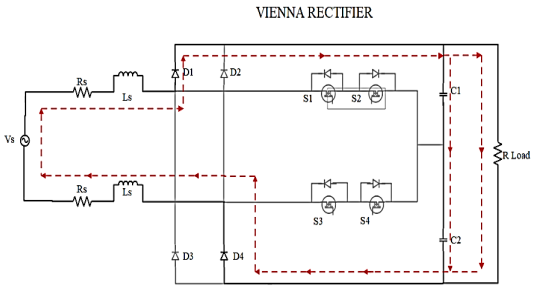

(b)

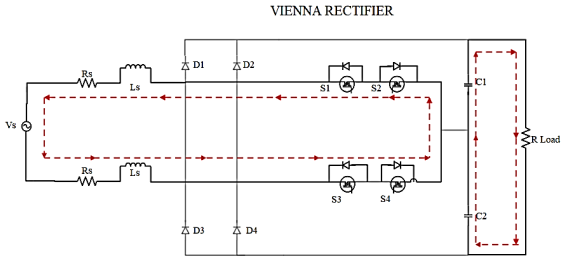

(c)

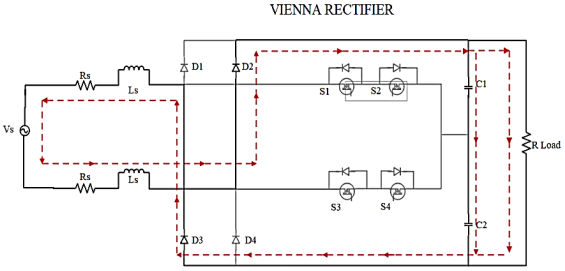

(d)

Fig. 2 – Mode 4 (switches are ON, and diodes D2 and D4 are ON).

In Mode 4, the diodes D2 and D3 are on, and the switches labeled S1, S2, S3, and S4 are off. The incoming current is negative in this mode. Figure 2d depicts the capacitors C1 and C2 and the inductors L1 and L2 while they are charging.

2.2. SLIDING MODE CONTROLLER

A nonlinear control strategy known as SMC controls a system's behavior reliably. The fundamental goal of SMC is to produce a sliding surface—a hyperplane that divides the system's desired behavior from its undesirable behavior—in the system's state space. The system trajectory must slide through this surface to execute the desired behavior. A function is known as the sliding function, which is intended to have a value of zero on the sliding surface, negative in value on one side of the surface, and positive on the other, which defines the sliding surface.

The sliding function was chosen to force the system's dynamics to slide through the surface toward the desired behavior. The SMC strategy entails creating a mechanism that generates command inputs to move the system trajectory toward the surface that slides and then maintain it there. The controller typically consists of two components: the reaching law, which pushes the entire structure to the sliding surface, and the sliding mode control law, which keeps the arrangement on the sliding surface.

The setup is accelerated as quickly as possible to the sliding surface using the reaching law, a high-gain control law. The sliding mode control maintains the process on the sliding

surface by producing control inputs that keep the sliding function at zero. The robustness of SMC to system uncertainties and disturbances is one of its main benefits. SMC is a well-liked option to regulate nonlinear systems with uncertainties because the sliding mode control law is created to dismiss modeling slips and disturbances. SMC can be difficult to use in practice because the high gain reaching law can lead to chattering quick switching between control inputs.

VR in a single phase is controlled by sliding mode control when the input voltage is average and distortion-free. Using the baseline voltage to correct power factors enables the resultant voltage to be changed to the desired level, minimizing steady-state errors and enhancing transient responses. A definition of the sliding surface B is:

$$B = \beta_1 s_1 + \beta_2 s_2 + \beta_3 s_3, \quad (1)$$

$$E = \frac{1}{2}\big(1 + \text{sign}(B)\big), \quad (2)$$

$$i_f = K v_{out}\big[v_f - v_{out}\big] = K \sin(\omega t)\big[v_f - v_{out}\big], \quad (3)$$

$$\begin{cases} s_1 = i_f - i_l, \\ s_2 = \big[v_f - v_{out}\big], \\ s_3 = \int [s_1 + s_2] \mathrm{d}t, \end{cases} \quad (4)$$

This is the definition of the sliding surface. B in terms of weighted sums of the sliding variables s_1, s_2 and s_3. The coefficients β_1, β_2 and β_3 is the weighting factor that determines the contribution of each sliding variable to the sliding surface.

Reference current and voltage are denoted by the letters i_f and v_f, respectively, and voltage error gain is denoted by the letter K. A high value for K is used to improve the dynamic reaction and lessen steady-state voltage errors.

$$s_1 = \frac{\mathrm{d}(i_f - i_l)}{\mathrm{d}t} = \omega K \cos(\omega t)\big[v_f - v_{out}\big] + \\ + K \sin(\omega t)\left[\frac{\mathrm{d}v_{out}}{\mathrm{d}t}\right] - \frac{v_s - \overline{uv_{out}}}{L}, \quad (5)$$

$$s_2 = \frac{\mathrm{d}(v_f - v_{out})}{\mathrm{d}t} = -\frac{\mathrm{d}v_{out}}{\mathrm{d}t}, \quad (6)$$

$$s_3 = s_1 + s_2 = K \sin(\omega t)\big[v_f - v_{out}\big] - i_l + v_f - v_{out}. \quad (7)$$

When using the SM controller, the comparable control signal for the Vienna rectifier is obtained by solving

$$\frac{\mathrm{d}B}{\mathrm{d}t} = \beta_1 s_1 + \beta_2 s_2 + \beta_3 s_3 = 0 \quad (8)$$

$$uv_{out} = \big[v_f - v_{out}\big]\left[L\omega K \cos(\omega t) + L\frac{\beta_3}{\beta_1} K \sin(\omega t) + L\frac{\beta_3}{\beta_1}\right] \\ - \frac{dv_{out}}{dt}\left[LK \sin(\omega t) + \frac{\beta_2}{\beta_1}\right] - \frac{\beta_3}{\beta_1} L i_l + v_{out} - v_s, \quad (9)$$

where

$$K_1 = L\omega K \cos(\omega t) + L\frac{\beta_3}{\beta_1} K \sin(\omega t) + L\frac{\beta_3}{\beta_1}, \quad (10)$$

$$K_2 = LK \sin(\omega t) + \frac{\beta_2}{\beta_1}, \quad (11)$$

$$K_3 = \frac{\beta_3}{\beta_1} L. \quad (12)$$

Assuming $v_{rip} = uv_{out}$ and substituting uv_{out} with v_{rp},

$$v_{rp} = K_1\big[v_f - v_{out}\big] - K_2 \frac{dv_{out}}{dt} - i_l + v_{out} - v_s, \quad (13)$$

$$v_{rip} = uv_{out}. \quad (14)$$

3. DESIGN OF PASSIVE COMPONENT

3.1. SIZING OF INDUCTOR

The inductor will reduce the harmonics in the switching frequency. The voltage across the inductor

$$v = L_i \frac{\mathrm{d}i}{\mathrm{d}t}. \quad (15)$$

The VR voltage equation is

$$\frac{V_{bus}}{2} - V_{rms} = L_i \times \frac{\Delta i_{pp}}{D*T}, \quad (16)$$

where L_i – Inductance; D – duty cycle; T - time, $T = \frac{1}{F_{sw}}$; F_{sw} – switching period; Δi_{pp} – change in current; m_a – modulation index.

$$\Delta i_{pp} = \frac{D \times T \times (\frac{V_{bus}}{2} - V_{rms})}{L_i}, \quad (17)$$

Assume $V_{rms} = D\frac{V_{bus}}{2}$, $D = m_a \times \sin(\omega t)$, then

$$\Delta i_{pp} = \frac{D \times T \times \frac{V_{bus}}{2}(1 - D)}{L_i}, \quad (18)$$

The ripple current can be derived as

$$\Delta i_{pp} = \frac{T \times \frac{V_{bus}}{2}(m_a \times \sin(\omega t) - {m_a}^2 \times \sin^2(\omega t))}{L_i}, \quad (19)$$

Differentiating eq. (19) yields

$$\frac{\mathrm{d}(\Delta i_{pp})}{\mathrm{d}t} = \frac{T \times \frac{V_{bus}}{2}(m_a \times \cos(\omega t) - 2{m_a}^2 \times \sin(\omega t)\cos(\omega t))}{L_i} = 0, \quad (20)$$

$$\sin(\omega t) = \frac{1}{2m_a}. \quad (21)$$

The maximum ripple can be obtained at $\sin(\omega t) = \frac{1}{2m_a}$ and substitute in eq. (20)

$$\Delta i_{pp} = \frac{\frac{V_{bus}}{2}{m_a}^2 T}{4{m_a}^2 L_i}, \quad (22)$$

$$L_i = \frac{\frac{V_{bus}}{2}}{4{m_a}^2 F_{sw} {m_a}^2 \Delta i_{pp_{max}}}. \quad (23)$$

The required inductance can be calculated by using eq. (23).

3.2. SIZING OF CAPACITOR

The capacitor reduces the DC output voltage ripples

$$C = \frac{1}{3}\left(\frac{P}{4 \times f \times (v^2 - (v - \Delta v)^2)}\right), \quad (24)$$

where f = grid side frequency, P = input power, Δv = change in source voltage.

4. RESULTS AND DISCUSSION

The VR simulation results for SMC are displayed in this section. The suggested system's simulation parameters are shown in Table 1.

Table 1
Parameter used for simulation

Parameter	Value
Source voltage	230 V
Resultant Voltage	400 V
Capacitor	2.5 µF
Inductor	5 mH
Line resistance	5 Ω
Grid Frequency	50 Hz

The output of this system is 400 V DC after being converted from 230 V AC. MATLAB/Simulink is employed to simulate the VR in a single phase depending on sliding mode control. Figure 3 depicts a simulation of the VR in a single phase depending on sliding mode control. In Figure 4, the supply voltage of 230 V is shown.

Figure 5 illustrates the proposed system's DC output voltage of 400 V and output current for a 230 V source voltage. This system is suitable for high-power applications. The DC side capacitor helps smooth out the resulting voltage and currents. According to Fig. 6, the input current's THD is 0.2%.

The suggested system reduces DC output voltage ripples and keeps the power factor close to unity. Mechanisms utilized for high-power applications introduce fewer harmonics to the supply side.

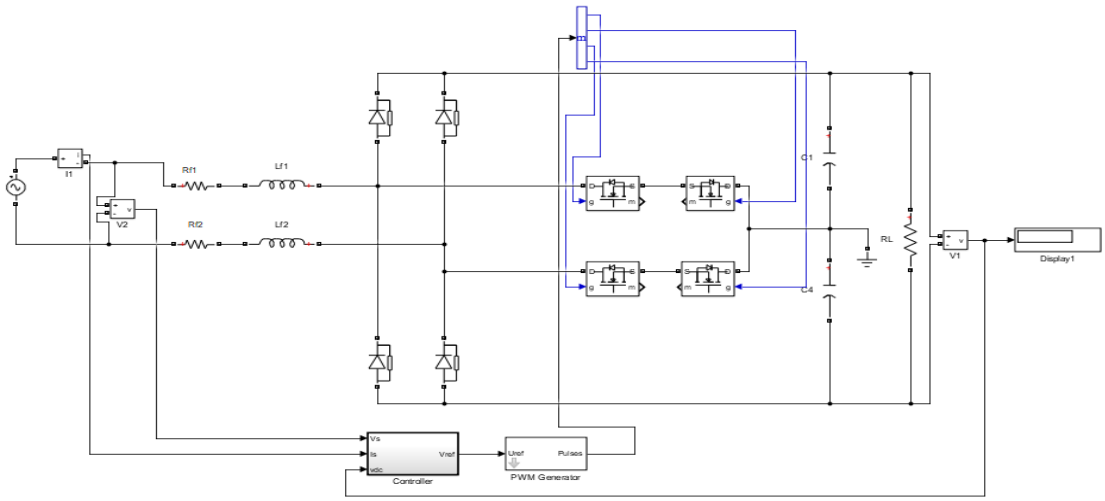

Fig. 3 – Single phase simulation diagram of VR-SMC.

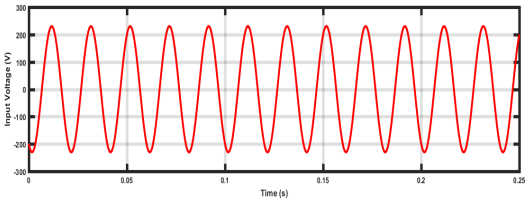

Fig. 4 – Source voltage waveform for 230 V_{AC}.

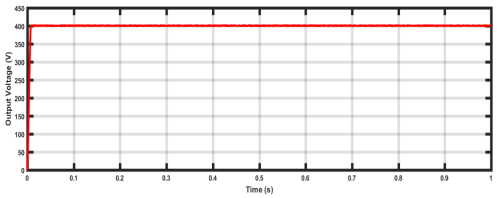

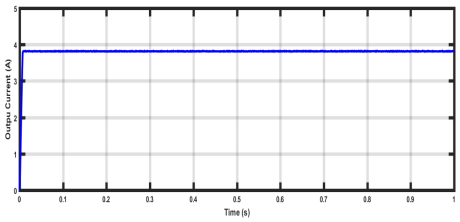

Fig. 5 – DC output voltage and current for 230V_{AC} and 400V_{DC}.

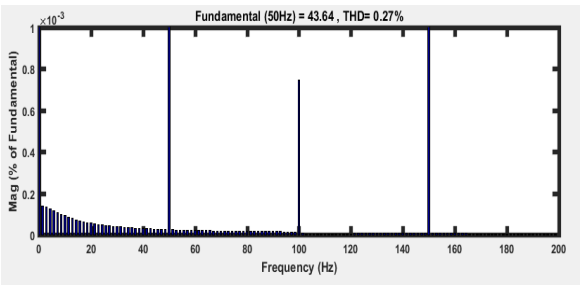

Fig. 6 – Input current's THD.

4.2. EXPERIMENTAL ANALYSIS

Figure 7 displays the hardware setup for the electric vehicle charging station, which includes the VR in a single phase depending on the sliding mode control. THD is measured with the aid of a power quality analyzer. The ripples are lessened by using the capacitor as a filter. The hardware component specifications are shown in Table 2 for your reference.

Table 2
Description of a hardware component

Components Name	Specifications
MOSFET	IRFP460 N-Channel
Optocoupler	PC817
Diode	MUR460
Inductor	5mH
Potential Transformer	6V, 500mA
Current Transformer	230V, 1A
Capacitor C1, C2	2.5µF, 440V

SMC on VR has been tested to deliver steady direct current voltage with low THD on the input side. The proposed system has a 230 V source voltage and a 400 V output voltage. VR's supply voltage waveform for 230 V with SMC is presented in Fig. 8. Figure 9 displays the amount of voltage onto the rectifier for a 400 V output and a 230 V input. Figure 10 displays the voltage throughout D1 and D3 for 230 V input and 400 V output, while Fig. 11 displays the voltage across D2 and D4.

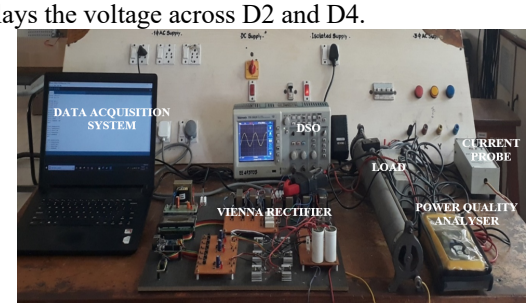

Fig. 7 – Overall hardware setup.

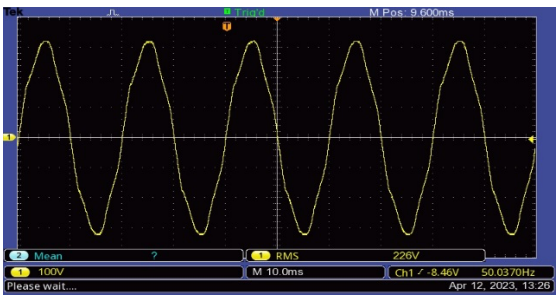

Fig. 8 – Source voltage waveform for 230 V_{AC}.

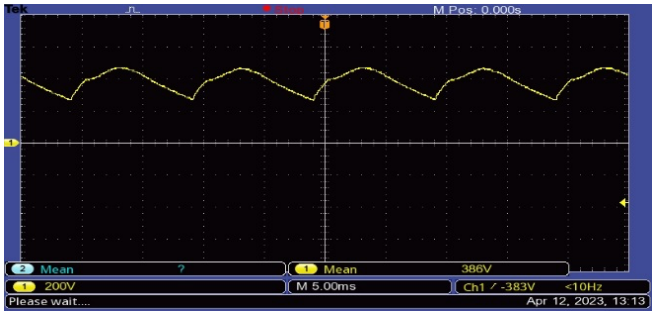

Fig. 9 – Voltage across the rectifier.

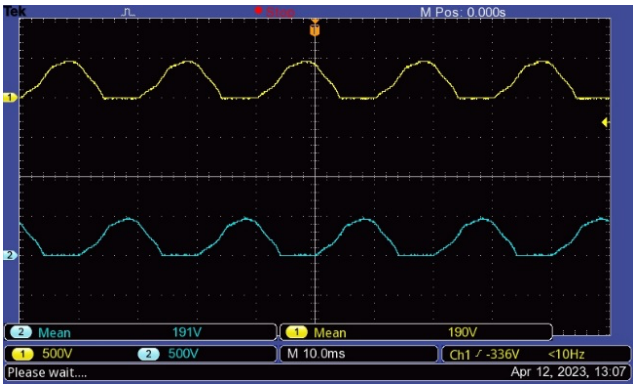

Fig. 1 – Voltage across the Diode D1 and D3.

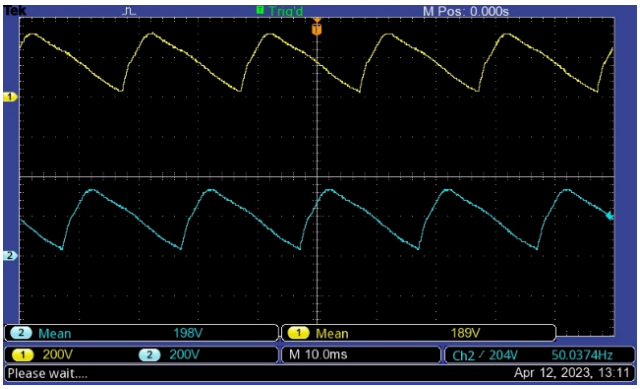

Fig. 1 – Voltage across the diode D2 and D4.

The voltage across the capacitors C1 and C2 is shown in Fig. 12, and the ripples are reduced by using these capacitors. Figure 13 depicts the output voltage, which is 400 V DC stable for 230 V input. Figure 14 displays the input current's %THD, which is 0.36. The proposed system has a high conversion efficiency and low input side harmonics. Figure 15 shows the various THD values for the different output powers. The range of THD values is 2.5% to 0.27%.

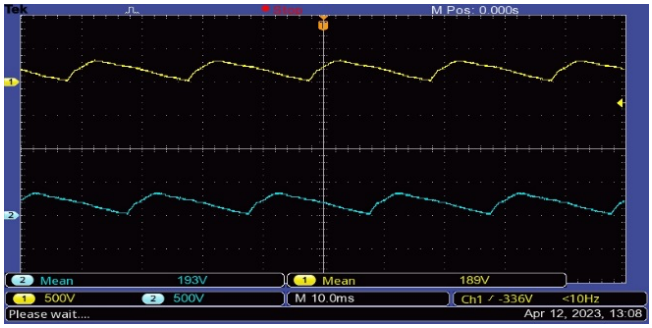

Fig. 12 – Voltage across the capacitor C1 and C2.

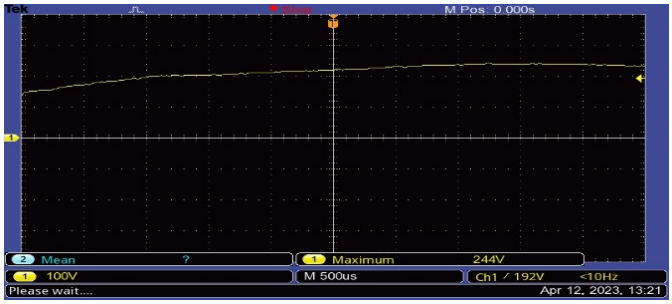

Fig. 13 – Output voltage.

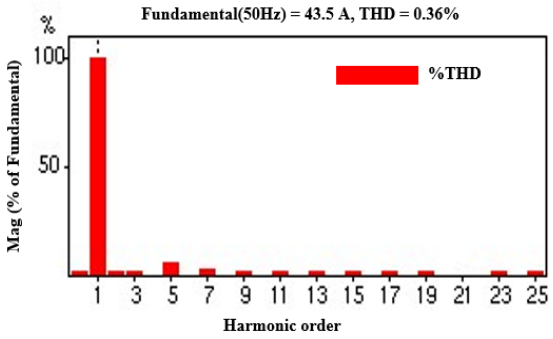

Fig. 14 – Input current's THD.

4.3. PERFORMANCE ANALYSIS

The comparisons between the proposed (Fig. 1) and conventional single-phase VRs [15] are listed in Table 3. In Table 3, ΔVprv is the peak value of the ripple voltage of output capacitor C1 (or C2), whose expression is

$$\Delta V_{prv} = \frac{P_o}{2\omega C_1 V_p}, \qquad)$$

where P_o is output power, and ω is the angular frequency of input voltage.

Table 3
Comparison between the proposed rectifier and conventional rectifier

Component	Conventional VR [15]	Proposed VR
Power switches	2	4
Power diodes	2	4
Output capacitors	2	2
Input Inductor	1	2
Ripple voltage of C1 or C2	$\Delta V_{prv}(\frac{2}{3}\pi + \sqrt{3})$	ΔV_{prv}
Range of output voltage	$> 2\sqrt{2}V_s$	$> \sqrt{2}V_s$

As can be seen in Table 3:

1) The proposed single-phase Vienna rectifier contains more power semiconductor components than the conventional single-phase Vienna, which raises the device's size and cost.

2) The voltage ripple of output capacitor C1 (or C2) in the conventional single-phase VR is $(2/3\pi + \sqrt{3})$ times greater than that in the proposed single-phase VR, indicating that the traditional single-phase VR requires a larger output capacitor and is therefore more expensive and larger.

3) The proposed VR's most significant benefit is the twice as wide output voltage range as the original single-phase VR.

A 230V, 1A current transformer is used in rectifier circuits to monitor or measure current, providing feedback to the control system (such as the sliding mode control in the VR diagram). The proposed VR's additional components (*e.g.*, extra switches and diodes) suggest that the transformer must handle more demanding electrical conditions.

Figure 16 illustrates the efficiency level for the maximum

output power, which ranges from 95% to 98%. Figure 17 displays the power factor as being maintained between 0.96 and 0.99. The suggested system can sustain an almost unity power factor. Table 3 compares the proposed system to the current system.

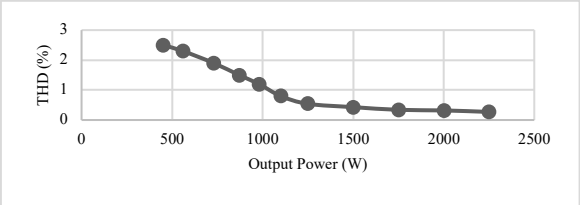

Fig. 15 – Curve of THD.

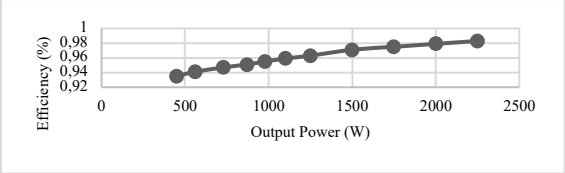

Fig. 16 – Curve of efficiency.

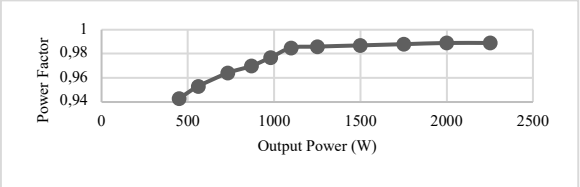

Fig. 17 – Curve of power factor.

Table 4
Performance evaluation between the proposed system and current systems.

Converter	Controller	%THD
Voltage source inverter	Sliding mode control [3]	1.4
Vienna rectifier	Hysteresis controller [12]	3.86
Vienna rectifier	Sliding mode control	0.36

In Table 4 proposed system's THD is lower than that of the current system. Consequently, the suggested system is more effective than the existing system.

5. CONCLUSION

This paper suggests a sliding mode control VR for an electric vehicle charging station. It is a reliable and effective approach for controlling the output voltage, and the combination of the VR topology and the sliding mode control technique provides the rectifier's current. The system power factor is maintained at unity, and harmonics on the input side are reduced. Simulations and experimental results have demonstrated the superiority of the suggested controller over the conventional PFC controller.

CREDIT AUTHORSHIP CONTRIBUTION

Banumalar Koodalsamy: Presented idea.
Vanaja Narayanaswamy: Theory and computations
Karthikeyan Krishnamoorthy: Results analysis
Bhuvanesh Ananthan: Simulations and results

Receive on 17 December 2023

REFERENCES

1. M.H. Islam. M.A. Razzak, *Power factor correction for single phase loads using modified Vienna rectifier*, 3rd International Conference on Electrical Engineering and Information Communication Technology (ICEEICT), pp. 1–6 (2016).
2. H. Komurcugil, S. Ozdemir, I. Sefa, N. Altin, O. Kukrer, *Sliding-mode control for single-phase grid-connected $\mbox{LCL}$-filtered VSI With double-band hysteresis scheme*, IEEE Transactions on Industrial Electronics, **63**, pp. 864–873 (2016).
3. G. Rubio-Astorga, J.D. Sánchez-Torres, J. Cañedo, A.G. Loukianov, *High-order sliding mode block control of single-phase induction motor*, IEEE Transactions on Control Systems Technology, **22**, pp. 1828–1836 (2014).
4. A. Mallik, J. Lu, A. Khaligh, *Sliding mode control of single-phase interleaved totem-pole PFC for electric vehicle onboard chargers*, IEEE Transactions on Vehicular Technology, **67**, pp. 8100–8109 (2018).
5. A.N. Arvindan, D.K. Akshay, E. Siby, K.M. Keerthana, *Efficacy of hysteresis current control in the single-phase Vienna rectifier topologies for improved power quality*, International Conference on Power and Embedded Drive Control (ICPEDC), pp. 318–325 (2017).
6. S. A. Shaon, K.M.A. Salam, *Study of Vienna rectifier and a highly efficient single phase two stage inverter with low THD*, 8th International Conference on Electrical and Computer Engineering, pp. 619–622 (2014).
7. U.K. Shinde, S.G. Kadwane, S.P. Gawande, M.J.B. Reddy, D.K. Mohanta, *Sliding mode control of single-phase grid-connected quasi-Z-Source Inverter*, IEEE Access, **5**, pp. 10232–10240 (2017).
8. S. Hou, J. Fei, Y. Chu, C. Chen, *Experimental investigation of adaptive fuzzy global sliding mode control of single-phase shunt active power filters*, IEEE Access, **7**, pp. 64442-64449 (2019).
9. B. Guo, M. Su, Y. Sun, H. Wang, H. Dan, Z. Tang, B. Cheng, *A robust second order sliding mode control for single-phase photovoltaic grid-connected voltage source inverter*, IEEE Access, **7**, pp. 53202–53212 (2019).
10. U.K. Kalla, B. Singh, S.S. Murthy, C. Jain, K. Kant, *adaptive sliding mode control of standalone single-phase microgrid using hydro, wind, and solar PV array-based generation*, IEEE Transactions on Smart Grid, **9**, pp. 6806–6814 (2018).
11. A. Kumar, D. Sarkar, P.K. Sadhu, *power quality improvement in induction heating system using Vienna rectifier based on hysteresis controller*, Electric Power Components and Systems, **48**, pp. 892–905 (2020).
12. J. Fei, Y. Chen, *Fuzzy double hidden layer recurrent neural terminal sliding mode control of single-phase active power filter*, IEEE Transactions on Fuzzy Systems, **29**, pp. 3067–3081 (2021).
13. A. Arpadžić, A. Bosović, A. Merzić, M. Musić, *Impacts of deregulated and regulated electric vehicle charging in a distribution network*, Rev. Roum. Sci. Techn. – Électrotechn. Et Énerg., **67***, 4*, pp. 451-456 (2022).
14. D. Ziane, A. Azib, A. Oubelaid, N. Taib, T. Rekioua, D. Rekioua, *Proposed power factor correction circuit based on the single-ended primary-inductor converter controlled by sliding mode control strategy used in an electric vehicle charging station*, Rev. Roum. Sci. Techn. – Électrotechn. Et Énerg., **67**, *3*, pp. 241–245 (2022).
15. Y. Yuan, Z. Zhang, *A single-phase Vienna rectifier with wide output Voltage Range*, IEEE Transactions on Transportation Electrification, **8**, pp. 3884–3895 (2022).